

# Simultaneous Adsorption of Poly(Vinylpyrrolidone) and Anionic Hydrocarbon/Fluorocarbon Surfactant from Their Binary Mixtures on Polystyrene Latex

Hidenori Otsuka,<sup>†,||</sup> Terry A. Ring,<sup>‡</sup> Jenq-Thun Li,<sup>§</sup> Karin D. Caldwell,<sup>§</sup> and Kunio Esumi<sup>\*,†</sup>

*Department of Applied Chemistry, Institute of Colloid and Interface Science, Science University of Tokyo, Kagurazaka, Shinjuku-ku, Tokyo 162-8601, Japan, Department of Chemical and Fuels Engineering, University of Utah, Salt Lake City, Utah 84112, and Center for Biopolymers at Interface, Department of Bioengineering, University of Utah, Salt Lake City, Utah 84112*

*Received: March 26, 1999; In Final Form: June 29, 1999*

Lithium dodecyl sulfate (LiDS)/lithium perfluorooctanesulfonate (LiFOS) and poly(vinylpyrrolidone) (PVP) were simultaneously adsorbed to polystyrene latex particles (PS) with diameter of 261 nm from PVP–LiDS and PVP–LiFOS binary mixed aqueous solutions. The conformation of PVP adsorbed on PS was estimated by using ESR. The thickness of the adsorbed layer was also determined by photon correlation spectroscopy (PCS) after pre-fractionation by sedimentation field-flow fractionation (sedFFF) which removed the aggregates and permitted an accurate PCS-based determination of the thickness of the coating layer. The adsorption of PVP was enhanced in the presence of LiDS at low LiDS concentrations owing to the formation of a surface complex of PVP and LiDS, followed by a decrease at high LiDS concentrations. A similar trend was observed in the PVP–LiFOS system. In both the PVP–LiDS and PVP–LiFOS systems, the conformation of PVP adsorbed was changed remarkably from loops and tails to trains with the surfactant concentration. The fraction of train segments in the PVP–LiFOS system was greater than that in the PVP–LiDS system, especially in the high surfactant concentration region. The thickness of PVP adsorbed on PS from the binary mixed solutions estimated from PCS decreased with an increase of the surfactant concentration. Thus, the ESR results were well correlated with the thickness of PVP adsorbed obtained from PCS.

## Introduction

The adsorption and orientation of polymers and surfactants, and their effects on the polymer conformation at the solid/liquid interface<sup>1–8</sup> are important to understand the mechanisms of stabilization and flocculation of dispersions and emulsions. The interactions between polymer and surfactant and the morphology of micelle–polymer complexes would affect the adsorption behavior at the solid/liquid interface. Although there are many factors influencing surfactant–polymer association, the effect of surfactant properties on the formation of the surfactant–polymer complex is of great interest. We reported<sup>7,9,10</sup> that poly(vinylpyrrolidone) (PVP) adsorption on colloidal particles such as alumina and hydrophilic/hydrophobic silica was significantly enhanced in the presence of anionic surfactants, where the conformation of PVP adsorbed estimated by ESR was markedly changed from loop or tail to train state. Of interest, in terms of the difference in hydrophobic group of surfactants, viz., hydrocarbon surfactant, lithium dodecyl sulfate (LiDS), and fluorocarbon surfactant, lithium perfluorooctanesulfonate (LiFOS), the fraction of train segments in the PVP–LiFOS system was greater than that in the PVP–LiDS system.

Adsorbed polymer layers have been characterized by several parameters such as the amount adsorbed, average thickness of the adsorbed layer, and fraction of bound segments. Reliable

information on the fraction of bound segments of adsorbed polymers can be obtained from various techniques including NMR<sup>11</sup> and ESR.<sup>12,13</sup> On the other hand, the thickness of the adsorbed polymer layer provides strong evidence in confirmation of the polymer conformation adsorbed on the solid surfaces.

On particulate particles, coating thicknesses are frequently analyzed by photon correlation spectroscopy (PCS).<sup>14</sup> As long as dust contamination can be minimized, the PCS technique offers a reliable and convenient way of determining the z-average of particle diameters present in a suspension, and the thickness of an adsorbed layer can, in principle, be determined from the size difference between coated and uncoated particles. For monodisperse populations, the PCS technique reproducibly yields diameters in good agreement with values from other well-accepted methods, such as analytical ultracentrifugation<sup>15,16</sup> and electron microscopy.<sup>17</sup> However, for polydisperse samples of unknown distribution the technique is less well suited as a characterization tool, as it only provides values for the average diameter together with a polydispersity index. Several comparative studies of polymer coatings on particles and on flat surfaces indicate a lack of agreement between coating thicknesses determined by PCS, on one hand, and by ultracentrifugation, ellipsometry, and neutron scattering on the other.<sup>18</sup> Various geometrical correction factors are applied to the non-PCS measurements to bring them into conformity with the PCS data, often with less than satisfactory results.<sup>19</sup>

To develop a better understanding of the question of polymer conformation on the surface of colloidal particles, we have used the field-flow fractionation(FFF), with the subtechnique of sedimentation(sed), to fractionate adsorbates into cuts of uniform particle size.<sup>20–22</sup> SedFFF is an elution method that has been

\* Corresponding author.

<sup>†</sup> Science University of Tokyo.

<sup>‡</sup> Department of Chemical and Fuels Engineering, University of Utah.

<sup>§</sup> Department of Bioengineering, University of Utah.

<sup>||</sup> Present address: Department of Materials Science, Graduate School of Engineering, The University of Tokyo, 7-3-1 Hongo, Bunkyo-ku, Tokyo 113-8656, Japan.

used extensively for the purification and characterization of colloidal materials. It is particularly the high inherent mass resolution and well-established relationship between retention and buoyant particle mass which are responsible for this use. If the goal of a particular experiment is separation, sedFFF is often the technique of choice because of its ability to generate fractions of well-resolved components. Owing to the uniformity of these cuts, PCS could be expected to give reliable information about the size of particles in each cut.

In this paper, we discuss the simultaneous adsorption of lithium dodecyl sulfate (LiDS)/lithium perfluorooctanesulfonate (LiFOS) and poly(vinylpyrrolidone) (PVP) from PVP–LiDS and PVP–LiFOS binary mixed solutions on polystyrene latex particles. The hydrodynamic thickness of the polymer–surfactant mixed layer on latex particles was also measured to confirm the relationship between the polymer conformation estimated by ESR and the thickness of the adsorbed layer obtained by PCS. Such latex particles are available in a variety of discrete and uniform sizes. The high level of cross-linking produced during the polymerization process causes these particles to behave as solid spheres with well-defined surface area. This makes them particularly useful as substrates in adsorption experiments intending to shed light on the surface concentration on the adsorbed component and the thickness of the adsorbed layer.

### Experimental Section

**Materials.** The spin-labeled PVP was prepared<sup>12</sup> by polymerizing *N*-vinyl-2-pyrrolidone (0.5 mol) and allylamine (0.11 mol) in ethanol, using *tert*-butylperbenzoate as an initiator, followed by a reaction with 4-isothiocyanato-2,2,6,6-tetramethyl-piperidinoxyl in dichloromethane at 40 °C. The spin-labeled PVP thus obtained was purified by repeated precipitations in diethyl ether. The molar ratio of *N*-vinyl-2-pyrrolidone to allylamine in the polymer determined by NMR was about 100:3. The molecular weight of the labeled polymer determined by static light scattering was about 16000.

Lithium dodecyl sulfate (LiDS) was synthesized from 1-dodecanol by sulfonation with chlorosulfonic acid, followed by neutralization with lithium hydroxide. After recrystallization from ethanol, the surfactant was purified by extraction with ether. Lithium perfluorooctanesulfonate (LiFOS) was synthesized and purified by a published method.<sup>23</sup> These surfactants were confirmed to be highly pure by the absence of a minimum in the surface tension. The critical micelle concentration values of LiDS and LiFOS, estimated from fluorescence spectra of pyrene-3-carboxaldehyde (PyCHO), in the presence of 10 mmol dm<sup>-3</sup> LiNO<sub>3</sub> were 4.1 and 4.0 mmol dm<sup>-3</sup> at 25 °C, respectively.<sup>24</sup>

Polystyrene latex standard (PS) with nominal diameter of 261 nm (Seradyn) was used as substrate in the adsorption experiments. Water used in this study was purified by passing it through a Milli-Q System (Nihon Millipore Co., Tokyo, Japan) until its specific conductivity fell below 0.1  $\mu\text{S cm}^{-1}$ .

**Methods and Measurements.** During the adsorption experiments, the polystyrene latex particles (2.5% (w/w)) were agitated with spin-labeled PVP and surfactant in aqueous solution of 10 mmol dm<sup>-3</sup> LiNO<sub>3</sub> for 24 h under constant end-over-end shaking at 25 °C. All the suspensions were adjusted to pH 7.0 by adding dilute solution of LiOH. The adsorbed amounts of spin-labeled PVP, LiDS, or LiFOS on PS were determined from the differences in concentrations before and after adsorption. The concentration of spin-labeled PVP was determined by ESR, while those of LiDS and LiFOS were determined by the Abbott method.<sup>25</sup>

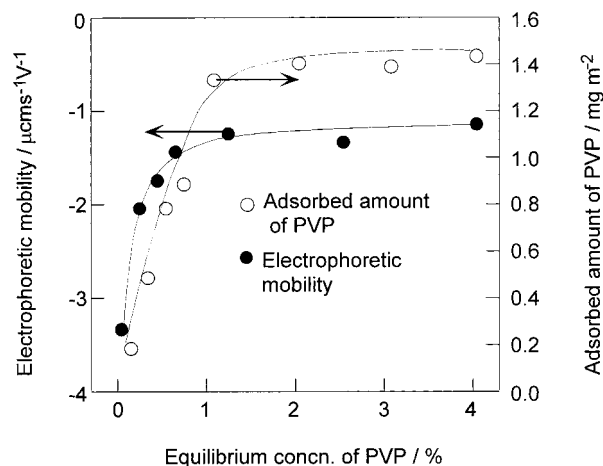


**Figure 1.** Adsorption of PVP on PS from PVP aqueous solution and electrophoretic mobility as a function of PVP concentration.

The ESR spectra were recorded on a JEOL JES FE 3-X spectrometer utilizing a 100-kHz field modulation and X-band microwaves. The slurries for the ESR measurements were prepared by centrifugation of the adsorption samples. Small amounts of polymer remained in the slurries but did not significantly affect ESR spectra at the solid/liquid interface.

The bare particles and particles coated with PVP/surfactant were sized by sedFFF. The sedFFF system was built in-house essentially according to the specifications used to construct the Model 100 particle fractionator from FFFractionation, Inc.; its flow channel has the following dimensions: length 96.0 cm, breadth 2.0 cm, and thickness 0.0254 cm for a measured void volume ( $V_0$ ) of 5.228 mL. The field strength used to accomplish sizing with this instrument was 1000 rpm, and the carrier flow was maintained at 2.3 mL min<sup>-1</sup> throughout. All reported sizes were the mean of at least three determinations made under identical conditions. For comparison, both bare particles and particle–polymer/surfactant composites were also sized by means of photon correlation spectroscopy using a Brookhaven Model BI90 fixed angle instrument. In these experiments it became necessary to include a filtration step before the actual sizing, since a certain amount of aggregates may appear to form in the adsorption process. In the filtration step, Millipore filter with a pore size of 1.0  $\mu\text{m}$  was used, and all liquids used for sample dilution were previously filtered through a 220 nm Millipore Millex GV filter. Each reported diameter was the mean of at least 10 observations.

All measurements were carried out at 25 °C.

### Results and Discussion

Figure 1 shows the adsorption isotherm of PVP on PS and electrophoretic mobility as a function of the equilibrium concentration of PVP. As can be seen, the PVP adsorption exhibits a strong affinity for the PS surface due to a sharp increase in the adsorption at low PVP concentrations and shows a nearly horizontal plateau in the concentration range of 1–4%. This strong affinity of PVP for the PS surface is probably owing to hydrophobic interaction. An increase in the adsorption of PVP makes the electrophoretic mobility of PS gradually decrease. The  $\zeta$  potential calculated from the electrophoretic mobility is an electrostatic potential at a shear plane distance away from the surface. The distance depends on the extent of the interaction of solvent molecules with the surface of the sample. For bare PS particles, the interaction with water extends up to a few layer of water molecules. The mobility of water molecules is restricted

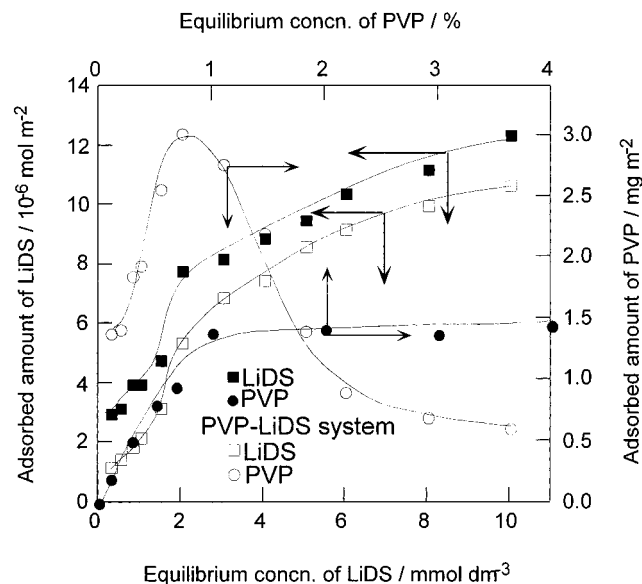


**Figure 2.** Adsorption of PVP and LiDS on PS from single and mixed aqueous solutions containing a fixed initial concentration of PVP ( $1.5 \text{ g dm}^{-3}$ ).

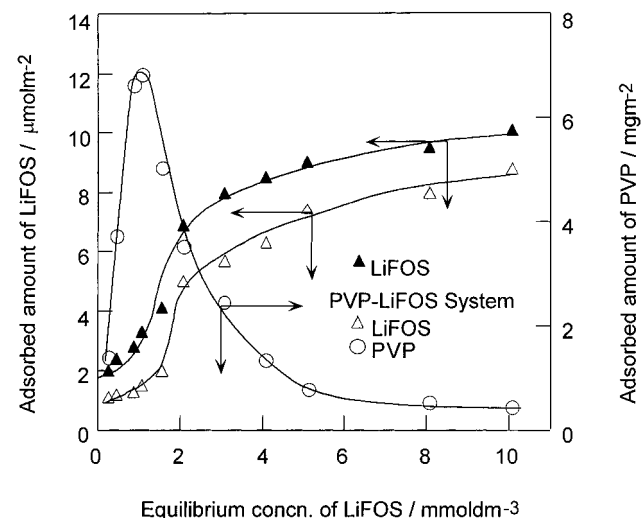


**Figure 3.** Adsorption of PVP and LiFOS on PS from single and mixed aqueous solutions containing a fixed initial concentration of PVP ( $1.5 \text{ g dm}^{-3}$ ).

by the polymer chain and the plane of shear distance is expected to be on the top of the PVP layer. Hence the PVP molecules would assume the conformation extended to the solution side with increasing adsorbed amount of PVP, which was confirmed by the measurement of layer thickness (discussed later).

Figures 2 and 3 show the simultaneous adsorption of PVP and anionic surfactants on PS from PVP–LiDS/PVP–LiFOS mixed aqueous solutions at constant feed concentration of PVP ( $1.5 \text{ g dm}^{-3}$ ) as a function of the surfactant concentration. In the case of surfactant alone, the amount of surfactant adsorbed was seen to increase gradually at low concentrations, but considerably at concentrations of surfactant above  $2 \text{ mmol dm}^{-3}$ . In both mixed systems, the adsorption of PVP increased sharply and showed a maximum, followed by a rapid decrease after passing a maximum, while the adsorbed amount of surfactant gradually increased. In addition, the adsorbed amount of surfactant in the presence of PVP was slightly lower than that in the absence of PVP for the whole range of surfactant concentrations studied. A similar result has been found for the systems such as LiDS/LiFOS–PVP–alumina<sup>7,9</sup> and LiDS/

LiFOS–PVP–hydrophilic/hydrophobic silica.<sup>10</sup> This enhancement in the PVP adsorption is probably due to the formation of complex between PVP and anionic surfactants.<sup>3,7,26</sup> It is well-known<sup>27–30</sup> that anionic surfactants interact with PVP, resulting in a formation of PVP–surfactant aggregates in aqueous solutions similar to polyelectrolytes. From the measurements of surface tension<sup>27</sup> and <sup>13</sup>C NMR spectroscopy,<sup>31</sup> it has been found that the formation of polymer–surfactant complexes, such as LiDS–PVP and SDS–PVP, is confirmed, and the basic structure of the complex in aqueous solution is also suggested<sup>31</sup> that the polymer molecules wrap around the aggregate, shielding hydrocarbon groups on the surface of the micelle from contact with water. In dilute surfactant solution with PVP, it seems likely that PVP attaches to the inner adsorbed layer of the surfactant, resulting in the formation of a PVP–surfactant complex on PS. Thus, hydrophobic interaction between the alkyl groups of the surfactant and the hydrophobic part of PVP chains takes place in the same manner as occurs in bulk solution. With increasing concentration of the surfactant, the adsorption of PVP rapidly decreases because PVP–surfactant complexes also start to form in the bulk solution, with the result that the surface is depleted from PVP, leaving room for extra surfactant to adsorb. On the basis of the mass action law, Gilanyi and Wolfram<sup>32</sup> concluded that, after the polymer–surfactant complex had formed, the activity of free surface-active molecules would decrease to some degree as the total concentration of surfactant in solution increased. Similar trends were observed for both PVP–LiDS and PVP–LiFOS systems. However, with the anionic surfactant concentration in the PVP–LiFOS system, the decrement in the adsorption of PVP after passing the maximum was much greater than that in the PVP–LiDS system. This implies that the PVP–surfactant complex in solution has a more favorable energy for LiFOS than for LiDS in bulk.<sup>27</sup> This is suggested by the fact that complexation of a fluorocarbon surfactant with polymer is different from that of a hydrocarbon surfactant, because the fluorocarbon chain has both hydrophobic and lipophobic properties.<sup>23,33</sup> This difference in the bulk properties between PVP–LiDS and PVP–LiFOS systems significantly reflected the adsorption of PVP; the enhancement of the adsorption of PVP for the PVP–LiFOS system was greater than that for the PVP–LiDS system. Thus, the difference in hydrophobic interaction between PVP–LiDS and PVP–LiFOS systems appeared more clearly on PS lattice, compared with the results previously reported.<sup>9,10</sup>

To elucidate the change in the conformation of PVP adsorbed on PS with increasing surfactant concentration, ESR spectra of spin-labeled PVP on PS were measured. The ESR spectra (spectra not shown) become broader with increasing LiDS or LiFOS concentration. For polymers adsorbed on the surface, a motionally narrowed spectrum is obtained if the label is attached to segments extending away from the surface into solution in the form of loops and tails. On the other hand, a broad anisotropic spectrum is obtained if the label is attached to trains of segments in contact with, or in close proximity to, the surface. Accordingly, as the surface coverage increases with increasing surfactant concentration, the PVP molecules adsorbed with the majority of their segments are close to the surface in trains. In addition, it is important to note that the ESR spectra of PVP–surfactant complex in aqueous solution are hardly altered compared to that of PVP alone.

The procedure for analyzing the ESR spectra is principally the same as those described previously.<sup>7</sup> The ESR spectra of the nitroxide spin label are very sensitive to the mobility of the given segment. When the motion is relatively fast (rotational



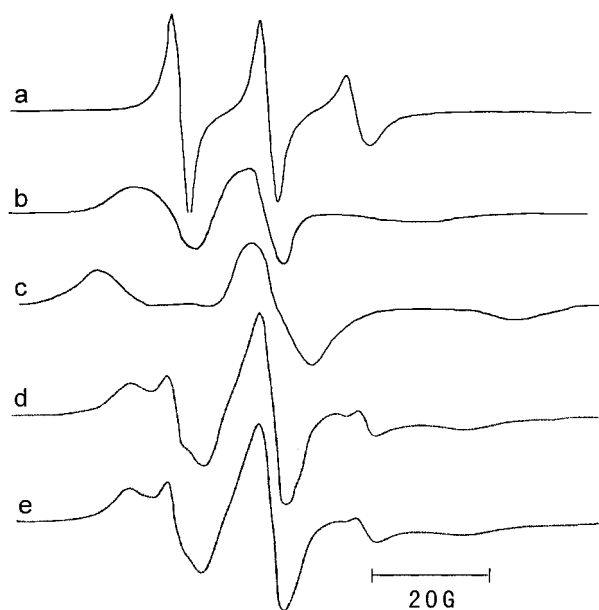


**Figure 4.** ESR spectra used for simulation of spin-labeled PVP adsorbed on PS. (a) unadsorbed in water at 25 °C, (b) at high temperature of 140 °C, (c) in the frozen solution at -120 °C, (d) adsorbed on PS in water at 25 °C, (e) reproduced by superposition of above three model spectra.

correlation time  $3 \times 10^{-9} \text{ s} > \tau_c > 3 \times 10^{-11} \text{ s}$ ), the spectrum consists of three well-resolved derivatives of Lorentzian lines which can be calculated completely theoretically using the very simple theory of Kivelson.<sup>34</sup> When the motion is slower, the shape of the spectrum is influenced by the anisotropic part of the spin Hamiltonian and new characteristic features appear which can be explained through the theory of Schneider and Freed.<sup>35</sup> The parameters of the spin Hamiltonian, the gyromagnetic tensor, and the hyperfine tensor have been determined using the solution spectrum and the rigid limit powder spectrum at the temperature of liquid nitrogen. At high temperature the motion is rather fast and the first kind of spectrum is the most important. At lower temperature, the motion becomes slow and the second kind of spectrum is detected. In an intermediate range, the spectrum appears as a superposition of the two precedent types and has been interpreted with a two-states model, analyzing both contributions and evaluating their respective weights with computer simulation. These two characteristic environments have been attributed to trains in close contact with the surface and rather immobilized and to loops and tails extending into a solution with rather fast motion. The ratio of the two populations corresponds to the ratio of the integrals of the absorption spectra that are characteristic for each environment.<sup>36</sup> On the basis of development of this two-states model, Sakai et al.<sup>13</sup> suggested that any composite ESR spectra can be separated into three components which may be assigned to signals from segments adsorbed in trains, short loops, and long loops or tails. We obtained three different spectra of PVP which have different degrees of motional freedom (Figure 4a–c). Apparently, the chain mobility decreased in the order of (a), (c), and (b). From the observation of the apparent line shape, the three spectra were found to correspond roughly to the three components of the adsorbed PVP, i.e. trains, loops, and tails. These three model spectra were superimposed upon one another (Figure 4e) with suitable intensity ratios to reproduce the observed spectrum (Figure 4d). The amplitude of each model spectrum was determined by a least-squares method involving multiple regression to fit a summation of the three spectra with the observed spectrum. In a three-component analysis, a close

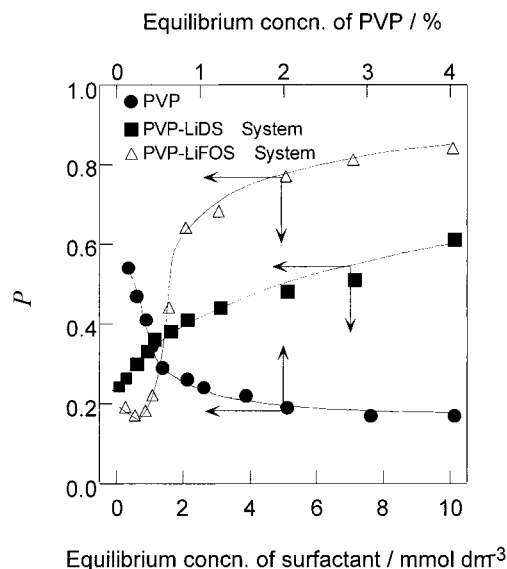


**Figure 5.** Plots of  $P$  values against PVP/surfactant concentrations. The fixed initial concentration of PVP is  $1.5 \text{ g dm}^{-3}$ .

curve fitting is found in every case, so that the ESR spectra of PVP adsorbed on PS surface are composed of three portions which have different local-chain mobilities, like those previously described for the adsorption of PVP on several surfaces.<sup>7,10</sup> In the PVP chain lying on the PS, the sequence of the segments directly bound to the surface should have restricted motion, whereas the detached segments should be more mobile. Consequently, the component in a very strongly immobilized state can be assigned to the train segments (Figure 4b), where the fraction of train segments is expressed as  $P$ . The other two components, in relatively mobile states, are assigned to the free segments having a short loop or a long loop (Figure 4a, c). It is noteworthy that the spin labels do not have a stronger affinity for the PS surface than the original vinylpyrrolidone monomer, indicating no strong adsorption or specific interaction with the PS surface. Hence it is thought that the spin label gives a reasonable representation of the polymer conformation at the PS/aqueous solution interface.

The values of  $P$  are given in Figure 5. The  $P$  value for the adsorption of PVP alone decreased monotonically with increasing PVP concentration, indicating that the conformation of adsorbed PVP molecules changes from trains to loops or tails. That is, the PVP molecules adsorbed on PS become considerably extended in the aqueous solution. Stuart et al.<sup>37</sup> compared the results obtained by Robb and Smith<sup>38</sup> with ESR and by Barnett et al.<sup>39</sup> with NMR. The recent NMR results must be considered particularly reliable, since residual solvent signal could be suppressed by an ingenious pulse sequence.<sup>40</sup> The agreement between the two methods is remarkably good, indicating that spin labeling has little or no consequence on the adsorption behavior of PVP on PS and gives reliable data on the conformation of PVP adsorbed on PS. On the other hand, for the PVP–surfactant systems the values of  $P$  increased steeply up to the concentration where the adsorption of PVP approached a maximum with increasing anionic surfactant concentration. This suggests that the conformation of adsorbed PVP molecules changes significantly from loops or tails to trains. This trend differs from the case in the absence of surfactant (PVP alone) which is in good agreement with the well-known relationship between surface coverage and conformation of the polymer; water-soluble polymers at low concentration adsorb at the interface with the majority of their segments close to the surface in trains, but as the concentration is increased, fewer segments

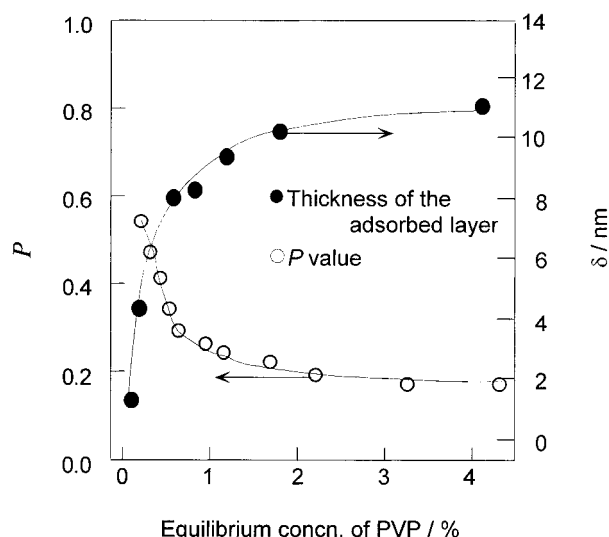


**Figure 6.** Relationship between the thickness of the adsorbed layer and  $P$  values for the PVP-PS system. The fixed initial concentration of PVP is  $1.5 \text{ g dm}^{-3}$ .

are located in the interface and most segments are extended normal to the interface as loop and as tail fragments.<sup>41</sup> It is noteworthy that despite the higher surface coverage, the majority of train segments are obtained in this study. This is probably because the PVP-surfactant complex is still formed by the interaction between PVP and the hydrophobic chain of the anionic surfactant on PS. Then, although the amount of PVP adsorbed decreased considerably, the values of  $P$  increased gradually, showing an increase of their segments in trains for both PVP-LiDS and PVP-LiFOS systems. However, there was a striking difference between two systems: the values of  $P$  for the PVP-LiFOS system increased more steeply and was greater than that for the PVP-LiDS system. This is because the PVP-surfactant complex has a more favorable energy and is less mobile for LiFOS than for LiDS.<sup>27</sup> A similar behavior in the change of  $P$  has been obtained<sup>7</sup> for PVP-LiDS/LiFOS system on alumina.

The hydrodynamic thickness,  $\delta$  (nm), of the polymer and polymer-surfactant mixed layer on PS was measured to confirm the relationship between the polymer conformation ( $P$  value) estimated by ESR and the thickness of the adsorbed layer. Figure 6 shows the layer thickness and values of  $P$  as a function of the PVP concentration when PVP from aqueous solution was adsorbed on PS. The adsorption layer thickness of PVP alone on the PS surface suggested that the molecules would be adsorbed flat on the surface in the very low concentration region, giving a thinner layer. When the PVP concentration increases, the adsorbed layer rapidly becomes thicker because larger loops and tails are formed. It is known<sup>42</sup> that at low PVP concentrations the typical conformation of PVP chain molecules at the solid/aqueous solution interface consists of a sequence of many short loops and trains and at higher coverage the bound fraction decreases due to the formation of a relatively dense loop layer, with a few long tails protruding into the solution as mentioned above. Adsorbed layer thickness in the range 5–10 nm (plateau adsorption region) are known in the case of Pluronic F68,<sup>43</sup> poly(ethylene oxide),<sup>44</sup> nonylphenyl poly(propylene oxide)-poly(ethylene oxide) adducts<sup>45</sup> and poly(vinylpyrrolidone),<sup>42</sup> which is consistent with our results. Further, hydrodynamic thickness of adsorbed polymer layers has been calculated by Stuart et al.<sup>46</sup> on the basis of a porous layer model using segment density profiles calculated with the Scheutjens-Fleer adsorption theory. Comparisons of the molecular weight and adsorbed amount

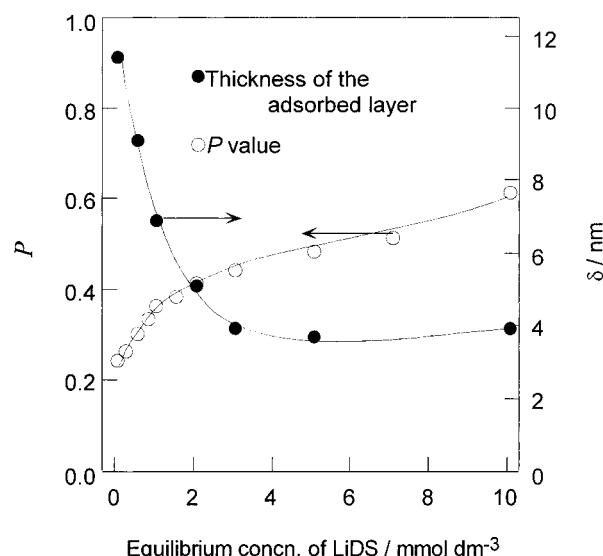


**Figure 7.** Relationship between the thickness of the adsorbed layer and  $P$  values for the PVP-LiDS-PS system. The fixed initial concentration of PVP is  $1.5 \text{ g dm}^{-3}$ .

dependence of the hydrodynamic thickness are made with experimental data obtained by photon correlation spectroscopy on a system of polystyrene latex particles dispersed in aqueous poly(ethylene oxide) solutions. It is confirmed that the dominant contribution to this thickness comes from long tails, which extend far into the solution. Thus, the thicker layer can be attributed to the PVP adsorbed as tails in this study. From the comparison of the layer thickness and the  $P$  values on PS latex and silica previously reported,<sup>10</sup> one can conclude that some influence of the energetic interactions on the hydrodynamic layer thickness and the  $P$  value exists;  $P$  value and layer thickness are obtained in the plateau region of the adsorption isotherm as follows— $P$ , 0.2;  $\delta$ , 12 nm on PS latex,  $P$ :0.7,  $\delta$ :10 nm on hydrophilic silica,<sup>10</sup>  $P$ :0.87;  $\delta$ :10 nm on hydrophobic silica,<sup>10</sup> respectively. The influence of the chemical nature of the surface can be explained if according to the Scheutjens-Fleer (S. F.) theory the hydrodynamic thickness is determined by the tail. The fraction of tail segments is strongly influenced by the net polymer-surface interaction energy. Therefore, we conclude that a smaller number of segments in the tails and a higher number of segments in the trains on the polar silica surface are due to the strong polymer-surface interaction than on the hydrophobic PS latex. Figures 7 and 8 show the layer thickness and values of  $P$  as a function of the surfactant concentration when PVP from PVP-surfactant mixed aqueous solution was adsorbed on PS. In Figure 7, a large decrease in the thickness of the adsorbed layer occurred with increasing LiDS concentration as the values of  $P$  increased, indicating that the conformation of PVP adsorbed on PS significantly affects the thickness of the adsorbed layer. The decrement in the thickness of the adsorbed layer with increasing surfactant concentration is greater for the PVP-LiFOS system than that for the PVP-LiDS system. Thus, the correlation between the layer thickness and the values of  $P$  confirms the conformation change in PVP in increased surfactant concentration.

## Conclusion

The simultaneous adsorption of PVP and LiDS/LiFOS on polystyrene latex particles was investigated. The adsorption of PVP showed a sharp increase at lower surfactant concentrations, and then decreased with increasing surfactant concentration. The

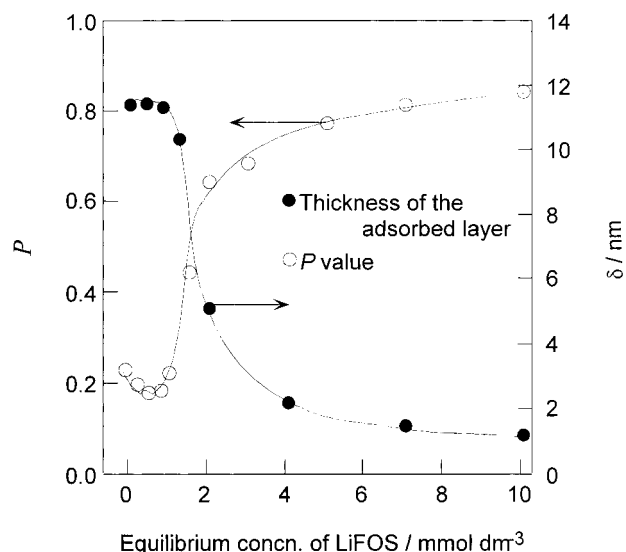


**Figure 8.** Relationship between the thickness of the adsorbed layer and  $P$  values for the PVP–LiFOS–PS system. The fixed initial concentration of PVP is  $1.5 \text{ g dm}^{-3}$ .

enhancement in the adsorption of PVP on polystyrene latex surface in the presence of surfactant occurred due to the formation of a PVP–surfactant complex on the surface. The anionic surfactant concentration in the PVP–LiFOS system for this decrement was much lower than that in the PVP–LiDS system as well as that in the case of alumina and silica. The  $P$  value in the PVP–LiFOS system increased steeply at a much lower concentration of the surfactant and was greater than that in the PVP–LiDS system. The thickness of the adsorbed layer was also determined by PCS after pre-fractionation by sedFFF. The thickness of the PVP–surfactant adsorbed layer on polystyrene latex decreased with increasing surfactant concentration. Accordingly the ESR results were well correlated with the thickness of PVP adsorbed obtained from PCS.

## References and Notes

- (1) Esumi, K.; Yokokawa, M. *J. Jpn. Soc. Colour Mater.* **1992**, 65, 142.
- (2) Esumi, K.; Masuda, A.; Otsuka, H. *Langmuir* **1993**, 9, 284.
- (3) Ma, C.; Li, C. *J. Colloid Interface Sci.* **1989**, 131, 485.
- (4) Maltesh, C.; Somasundaran, P. *J. Colloid Interface Sci.* **1992**, 153, 298.
- (5) Tanaka, R.; Williams, P. A.; Meadows, J.; Phillips, G. O. *Colloids Surf.* **1992**, 66, 63.
- (6) Esumi, K.; Oyama, M. *Langmuir* **1993**, 9, 2020.
- (7) Otsuka, H.; Esumi, K. *Langmuir* **1994**, 10, 45.
- (8) Kilau, H. W.; Volts, J. I. *Colloids Surf.* **1991**, 57, 17.

- (9) Otsuka, H.; Esumi, K. *J. Colloid Interface Sci.* **1995**, 170, 113.
- (10) Otsuka, H.; Esumi, K.; Ring, T. A.; Li, J. T.; Caldwell, K. D. *Colloids Surf.* **1996**, 116, 161.
- (11) Cosgrove, T.; Griffith, P. C. *Adv. Colloid Interface Sci.* **1992**, 42, 175.
- (12) Fox, B. K. K.; Robb, I. D.; Smith, R. J. *Chem. Soc., Faraday Trans. 1* **1974**, 70, 1186.
- (13) Sakai, H.; Asakura, T.; Suzuki, K.; Horie, K. *Bull. Chem. Soc. Jpn.* **1981**, 54, 2180.
- (14) Killmann, E.; Maier, H.; Kaniut, P.; Gutling, N. *Colloids Surf.* **1985**, 15, 261.
- (15) Fontana, B. J.; Thomas, J. R. *J. Chem. Phys.* **1961**, 65, 480.
- (16) Cohen, Y.; Metzner, A. B. *Macromolecules* **1982**, 15, 1425.
- (17) Bradfood, B.; Vanderhoff, J. W. *J. Appl. Phys.* **1955**, 26, 864.
- (18) Garvey, M. J.; Tadros, T. F.; Vincent, B. J. *Colloid Interface Sci.* **1976**, 55, 440.
- (19) Killmann, E.; Maier, H.; Baker, J. A. *Colloids Surf.* **1988**, 31, 51.
- (20) Li, J. T.; Caldwell, K. D. *Langmuir* **1991**, 7, 2034.
- (21) Tan, J. S.; Butterfield, D. E.; Voycheck, C. L.; Caldwell, K. D.; Li, J. T. *Biomaterials* **1993**, 14, 823.
- (22) Li, J. T.; Caldwell, K. D.; Machtle, W. J. *Chromatogr.* **1990**, 517, 361.
- (23) Suzuki, T.; Esumi, K.; Meguro, K. *J. Colloid Interface Sci.* **1983**, 93, 205.
- (24) Esumi, K.; Otsuka, H.; Meguro, K. *J. Colloid Interface Sci.* **1990**, 136, 224.
- (25) Abbott, D. C. *Analyst* **1962**, 87, 286.
- (26) Ma, C. *Colloids Surf.* **1985**, 16, 185.
- (27) Nojima, T.; Esumi, K.; Meguro, K. *J. Am. Oil Chem. Soc.* **1992**, 69, 64.
- (28) Lange, H. *Kolloid Z. Z. Polym.* **1971**, 243, 101.
- (29) Fadnavis, N. W.; Engbert, J. B. F. N. *J. Am. Chem. Soc.* **1984**, 106, 2636.
- (30) Robb, I. D. In *Anionic Surfactants in Physical Chemistry of Surfactant Action*; Lucassen-Reynders, E. H., Ed.; Dekker: New York, 1981; p 109.
- (31) Chari, K.; Lenhart, W. C. *J. Colloid Interface Sci.* **1990**, 137, 204.
- (32) Gilanyi, T.; Wolfram, E. *Colloids Surf.* **1981**, 3, 181.
- (33) Muto, Y.; Asada, M.; Takasawa, K.; Esumi, K.; Meguro, K. *J. Colloid Interface Sci.* **1988**, 124, 632.
- (34) Kivelson, D. *J. Chem. Phys.* **1960**, 33, 1107.
- (35) Schneider, D. J.; Freed, J. In *Bimaterial Magnetic Resonance*; Berliner, L. J., Reuben, J., Eds.; Plenum: New York, 1989; Vol. 8.
- (36) Hommel, H.; Legrand, A. P.; Ben Ouada, H.; Bouchriha, H.; Balard, H.; Papirer, E. *Polymer* **1992**, 33 (1), 181.
- (37) Stuart, M. A. C.; Fleer, G. J.; Bijsterbosch, J. *J. Colloid Interface Sci.* **1982**, 90, 321.
- (38) Robb, I. D.; Smith, R. *Eur. Polym. J.* **1974**, 10, 1005.
- (39) Barnett, K. G.; Cosgrove, T.; Vincent, B.; Sissons, D. S.; Stuart, M. A. C. *Macromolecules* **1981**, 14, 1018.
- (40) Cosgrove, T.; Barnett, K. G. *J. Magn. Reson.* **1981**, 43, 15.
- (41) Glass, J. E. *Water-Soluble Polymers, Beauty with Performance*; American Chemical Society, Washington, DC, 1986; p 85.
- (42) Stuart, M. A. C.; Mulder, J. W. *Colloids Surf.* **1985**, 15, 49.
- (43) Kayes, J. B.; Rawlins, D. A. *Colloid Polym. Sci.* **1979**, 257, 622.
- (44) Koopal, L. K.; Hladý, V.; Lyklema, J. *J. Colloid Interface Sci.* **1988**, 121, 49.
- (45) Stuart, M. A. C.; Boomgaard, Th. van den; Zourab, S. M.; Lyklema, J. *Colloids Surf.* **1984**, 9, 163.
- (46) Stuart, M. A. C.; Waajen, F. H. W. H.; Cosgrove, T.; Vincent, B.; Crowley, T. L. *Macromolecules* **1984**, 17, 1825.